Next Nanotechnology 10 (2026) 100809

Contents lists available at ScienceDirect

Next Nanotechnology

journal homepage: www.sciencedirect.com/journal/next-nanotechnology

Research article

Toward sustainable food encapsulation: Eco-innovative and energy-efficient fabrication of phospholipid-stabilized nanoemulsions

Amrita Chakraborty [a,b], Niloy Chatterjee [c,e], Aatrayee Das [d], Sanjit Dey [b,e], Supratim Ghosh [f], Pubali Dhar [a,e,*]

[a] Laboratory of Food Science and Technology, Food and Nutrition Division, University of Calcutta, 20 B Judges Court Road, Kolkata, West Bengal, 700027, India
[b] Department of Physiology, University of Calcutta, 92, Acharya Prafulla Chandra Road, Kolkata, West Bengal, 700009, India
[c] SNM Scinovotech Pvt. Ltd., 1034 Madurdaha, East Kolkata Township, Kolkata, West Bengal, 700109, India
[d] Department of Chemical Engineering, Indian Institute of Technology, Kharagpur, West Bengal, 721302, India
[e] Centre for Research in Nanoscience & Nanotechnology, University of Calcutta, JD-2, Sector III, Salt Lake City, Kolkata, West Bengal, 700 098, India
[f] Department of Food and Bioproduct Sciences, University of Saskatchewan, 51 Campus Drive, Saskatoon, SK, S7N 5A8, Canada

ARTICLE INFO

Keywords:
Nanoemulsion
Soy-phospholipid
Sesame oil
Homogenization-evaporation
Physical stability
Oxidative stability
Lipolysis

ABSTRACT

The primary objective of the present venture is to fabricate food-grade phospholipid-stabilized oil-in-water nanoemulsion for the encapsulation of lignan-rich sesame oil. A large number of high-energy, high-cost instruments are available on the market; however, a combination of high-speed homogenization and the solvent evaporation method was successfully applied in this study to overcome the significant economic burden imposed by high-energy approaches. Furthermore, the challenge remained in circumventing synthetic surfactants and incorporating phospholipids as emulsifiers in the present work. The three nanoemulsion formulations, NEA, NEB, and NEC, were successfully fabricated using phospholipid and Tween 20 in 2:1, 1:1, and 1:2 ratios, respectively. The formulations were found to possess nano-droplet sizes, narrow polydispersity indices, and sufficient physical stability against creaming and phase separation. Phospholipid was shown to provide a thickened viscoelastic layer around the droplet, a highly negative surface potential and a favourable packing parameter. Engaging Tween 20 in adequate amounts was found to impart a steric-repulsive barrier to these phospholipid-stabilized formulations, which might help maintain stability across a wide range of pH and ionic strength. The physical stability against environmental stressors was highest in NEC owing to the substantial presence of Tween 20. On the contrary, NEA offered maximum protection against lipid peroxidation owing to the inherent antioxidant properties of phospholipids. Lipolysis in a simulated gastrointestinal environment was higher in the NEA formulation, indicating how interfacial composition alters enzyme kinetics under dynamic conditions. In this endeavour, selecting emulsifiers at the interface provides a platform that modulates physical and oxidative stability, as well as the *in vitro* digestion profile. The insights gained from this study yielded promising outcomes in the frontier area of nanodelivery.

1. Introduction

To accommodate the growing consumer demand for maximizing the bioavailability of natural products, nanoemulsion-based delivery vehicles have garnered keen interest due to their nanometric droplet size, increased surface area-to-volume ratio, site-specific targeting, and ability to overcome physiological barriers [1]. Oil-in-water (O/W) nanoemulsions (NEs), comprising tiny oil droplets dispersed in an aqueous phase, are considered an efficacious delivery tool for lipophilic bioactives due to their improved kinetic stability, controlled release, and satisfactory lipid digestibility [2].

Two primary approaches have been used to fabricate NEs: high- and low-energy methods. High-energy techniques widely used in the food industry typically rely on intense disruptive energy applied via expensive, specialized equipment, resulting in significant manufacturing costs [3]. On the contrary, low-energy approaches commonly leverage the system's inherent physicochemical properties, controlling interfacial phenomena rather than external mechanical forces [4]. A keen interest

* Corresponding author at: Centre for Research in Nanoscience & Nanotechnology, University of Calcutta, JD-2, Sector III, Salt Lake City, Kolkata, West Bengal 700 098, India.
E-mail addresses: pdhomesc@caluniv.ac.in, pubalighoshdhar@yahoo.co.in (P. Dhar).

https://doi.org/10.1016/j.nxnano.2026.100809
Received 10 April 2026; Received in revised form 22 June 2026; Accepted 22 September 2026
Available online 12 October 2026
2949-8295/© 2026 The Authors. Published by Elsevier Ltd. This is an open access article under the CC BY license (http://creativecommons.org/licenses/by/4.0/).

has developed among neo-age researchers in utilizing low-energy methods on a large scale due to their cost-effective productivity. However, a crucial drawback of low-energy techniques is the need for larger amounts of synthetic surfactants than those of high-energy techniques [5]. There is strong inertia in the food industry regarding the use of commercial synthetic surfactants, particularly due to cost, taste, and toxicity concerns. Furthermore, low-energy technology is limited in its applicability to systems that use natural emulsifiers, such as proteins, polysaccharides, or phospholipids, due to the high molecular weight and slow adsorption kinetics of these emulsifiers [6]. In the current scenario, to corroborate the perception of a safe, natural, non-toxic nano-delivery system, hybrid approaches that combine high-energy emulsification with low-energy solvent evaporation have been widely used in recent years [7]. The choice of biomaterials as emulsifying agents is attributable to their unique characteristics, including natural biodegradability, biocompatibility, sustainability, and eco-friendly attributes [8]. Moreover, phospholipids are widely used due to their amphiphilic nature, which includes a hydrophilic head group and two hydrophobic tails, allowing them to adsorb at the oil-water interface and readily stabilize emulsions [9]. Natural phospholipids have recently been reported to be effective in fabricating various NE formulations using high-energy techniques [10–12].

From this perspective, the core novelty and innovation of our study lies in the unique triad of an eco-innovative emulsifier composition, drastic energy-efficiency gains, and interfacial process optimization strictly tailored for food-grade, lipid-based delivery vehicles. The distinction of our work from conventional ventures rests upon three pillars. 1. Process optimization and mechanical simplification: Our strategy is to successfully fabricate stable nanoemulsions (hydrodynamic diameter of 60–90 nm) using only a standard rotor-stator high-speed homogenizer (HSH) instead of a high-pressure homogenizer (HPH). High-speed homogenizers are standard, low-cost baseline equipment in food laboratories and factories. High-speed homogenization followed by solvent evaporation is expected to increase the scalability of NEs for industrial production in developing countries, enabling efficient and economical meeting of consumer demand. 2. Compositional synergy at the interface (Asolectin–Tween 20): The breakthrough lies in the dual-stabilization nature of an all-natural structural scaffold composed of soy-phospholipid mixtures (asolectin) and Tween 20 in various combinations. The findings focus on the outstanding electrostatic stabilization imparted by phospholipids and the steric stabilization provided by Tween 20. 3. Impact on physical stability and lipid digestibility: The current venture indicates that modulating the interfacial composition and emulsifier concentration results in a remarkable alteration in physical stability in various conditions and *in vitro* lipid digestibility in the simulated digestive model. The facts and facets obtained from this analysis may help select the appropriate emulsifier and more conveniently optimize the fabrication technology for the future formulation of food-grade NEs.

2. Materials and methods

2.1. Materials

Commercially available sesame oil was purchased from the local market of Kolkata, India. Asolectin (mixture of phospholipids from soybean), synthetic surfactant Tween 20 and Nile red dye were procured from Sigma-Aldrich, MO, USA. All other chemicals and solvents used were of reagent grade.

2.2. Measurement of interfacial tension

The Interfacial Tension of Sesame oil/ Ethyl acetate/ emulsifier (phospholipid and Tween 20 in different ratios) was measured using a semi-automatic tensiometer (Lauda TD2, GmbH & Co., Germany) with a Du Noüy ring (20 mm diameter) [13].

2.3. Fabrication of NE using a combined homogenization and solvent evaporation approach

NEs were fabricated using a combined emulsification and solvent-evaporation approach, as described in a previous report [7], with slight modifications. To prepare an NE, a 10% (w/w) dispersed organic phase and a 90% (w/w) continuous aqueous phase were used. The dispersed phase consisted of 7.5% (w/w) ethyl acetate, 2.5% (w/w) sesame oil, and 1.8% (w/w) emulsifier in a 5 mM sodium phosphate buffer (pH 7.0) solution containing 0.02% (w/w) sodium azide. Asolectin (a mixture of Soy phospholipids) was blended with Tween 20 at three ratios (2:1, 1:1, and 1:2) to identify the optimal emulsifier combination. First and foremost, a coarse oil-in-water emulsion was prepared by adding the dispersed phase to the continuous phase under constant agitation at 2000 rpm for 2 h, using a magnetic stirrer. Second, the coarse emulsion was homogenised at 10,000 rpm using a T-18 digital Ultra-Turrax (IKA) high-speed homogeniser in the presence of an ice sheath for 30 min to minimize heat generation and lipid oxidation. Finally, the ethyl acetate solvent was removed using a rotary evaporator (Buchi model R-100) for 20 min at 45 °C. The fabricated NE was then stored in a freezer (4–8°C) for further use.

Following solvent evaporation and mass balance, a measured amount of water was added to the fabricated NE to maintain the final concentrations of oil and emulsifier in the system as before. The surfactant composition of formulations is given below (Tables 1 and 2):

2.4. Droplet size and electrical charge measurements

8-week storage stability at 25°C was assessed by measuring the hydrodynamic diameter and zeta potential of the droplets using a Malvern Nano ZS (Malvern Instruments, Zetasizer version 6.00, UK) [14,15].

2.5. Transmission electron microscopy (TEM)

The morphology of NEs was examined using negative-staining electron microscopy to measure particle size and shape directly. The images of the formulations were obtained using TEM (JEM-1010, JEOL, Tokyo, Japan) [16].

2.6. Stability of nanoemulsion under various pH and ionic conditions

The stability of NEs under various pH and ionic strength conditions was evaluated using their visual appearance and mean hydrodynamic diameter. The changes were studied after incubating the NEs in separate test tubes at several pH levels (3−8) and various ionic concentrations (0–500 mM) for 24 h at ambient room temperature (25 °C) [7]

2.7. Lipid oxidation measurements

TBARS measured oxidative stability of the encapsulated oil (2.5% w/w) in the NE systems during storage [17]. 2 mL samples were added to TCA (trichloroacetic acid)-TBA-HCl solution, which was prepared by mixing 75 g of TCA, 1.68 g of TBA, 8.8 mL of 12 M HCl, and 414 g of H2O. Next, 100 mL of TCA-TBA-HCl solution was added to 3 mL of 2% (w/w) butylated hydroxytoluene (BHT) in ethanol. TBARS, a pink chromogen, was formed, and the absorbance was measured at 532 nm using a spectrophotometer (GenesysTM 180 U; Thermo Scientific, Waltham, MA) against an appropriate reagent blank. Concentrations of

Table 1
Surfactant composition of the formulations NEA, NEB and NEC.

NE	Asolectin (w/w %)	Tween 20 (w/w %)
NEA	1.2	0.6
NEB	0.9	0.9
NEC	0.6	1.2

Table 2
Size-distribution of the particles of the formulations NEA, NEB, and NEC at the initial week concerning diameter, polydispersity index and zeta potential; results were stated as Mean ± SD (n = 3).

NE formulations (0 weeks)	Mean hydrodynamic diameter (nm)	Polydispersity Index	Zeta potential (mV)
NEA	76.24 ± 12.56	0.26 ± 0.03	-44.2 ± 1.31
NEB	69.89 ± 6.56	0.23 ± 0.05	-41.1 ± 1.76
NEC	67.12 ± 3.87	0.25 ± 0.02	-40.4 ± 2.53

TBARS were deduced from the standard curve prepared using 1, 1, 3, 3-tetraethoxypropane.

2.8. In-vitro digestion and determination of lipid digestibility

The lipid digestibility of NE formulations (NEA, NEB, and NEC) was comparatively analysed using a three-stage simulated in vitro digestion method, as per the earlier protocol with necessary alterations [18]. To prepare the simulated mouth phase, NaCl (0.1594 gm), KCl (0.0202 gm), and mucin (0.02 gm) were mixed with 10 mM phosphate buffer to bring the total weight to 100 gm. The pH was adjusted to 6.8. A 20 mL aliquot of the fabricated formulation was taken and blended with simulated salivary juice in equal proportions. The mixture was then placed in a temperature-controlled bath at 37°C and continuously agitated at 100 rpm for 5 min. To prepare simulated gastric juice, NaCl (2 gm) and 7 mL of HCl (35.5%) were mixed in 1 L of water. 0.32 wt% pepsin was further added to the mixture. The pH was adjusted to 1.5 using 1.0 M HCl. A 20 mL aliquot of the sample was taken from the simulated mouth phase and added to the simulated gastric fluid in equal volumes. Next, the pH was adjusted to 2.5 using 1 M NaOH. Finally, the mixture was placed over a magnetic stirrer for 2 h, and the temperature was maintained at 37℃. A 30 mL aliquot of the gastric sample was further incubated at 37°C, and the pH was adjusted to 7.0 with 1 M NaOH. After that, 1 mL of CaCl2 (110 mg/mL) and 4 mL of bile extract (46.87 mg/mL) were mixed with the solution. Finally, 2.5 mL of freshly prepared lipase solution (24 mg/mL) was added to the mixture for preparing the intestinal phase. The pH of the intestinal sample was maintained at 7.0 by adding 0.1 M NaOH dropwise to neutralise the FFA released during intestinal digestion. The temperature at this stage was maintained at 37 °C using a thermostatic bath with continuous agitation at 400 rpm. The volume of NaOH required to neutralise the FFA produced during intestinal digestion was noted. Beakers containing the raw NE formulations, left at 37 °C for 10 min, were used as the initial, or raw, phase.

2.8.1. Free fatty acid release

The amount of free fatty acids (FFA) released from NE was estimated using a titration method [2,19] to measure the digestive activity. Acetone (10 mL) was added to a sample volume (5 mL) of the mouth phase, gastric phase and intestinal phase to quench the enzymatic activity. Thereafter, 2–3 drops of a 1% (w/v) phenolphthalein indicator solution were added to the mixture. A direct titration with 0.1 mol·L-1NaOH using a burette was carried out. The percentage of free fatty acids released was determined using the following equation.

$$\% \text{ FFA} = 100 \times (v\text{NaOH} \times m\text{NaOH} \times M\text{lipid}) / w\text{lipid} \times 2$$

Where *v*NaOH is the volume of sodium hydroxide required to neutralise the FFA generated (in L), *m*NaOH is the molarity of the sodium hydroxide used (in mol·L-1), *w*lipid is the total weight of sesame oil initially present, and *M*lipid is the molecular weight of the sesame oil (1103.8 g· mol-1).

2.8.2. Confocal microscopy before and after digestion

A comparative analysis of the microstructures of oil droplets in the NEs, both before and after digestion, was conducted using a confocal scanning laser microscope (EVOS M5000 Imaging system, Thermo Fisher Scientific, USA) at 40X magnification [2,20]. Samples were stained with Nile Red (9-diethylamino-5H-benzo[α]phenoxazine-5-one, 0.25 mg mL-1 in dimethyl sulfoxide, 1:10 (dye: sample, v/v)), thereby making the oil droplets visible. A minute amount of the stained NE formulation was placed on a concave glass slide and covered with a glass coverslip to prepare the slide for confocal microscopy, which was fitted with an argon laser (excitation wavelength: 488 nm; emission wavelength: 500 nm).

2.9. Statistical analysis

All investigations were performed in triplicate using fabricated NE samples, and the results were represented as the mean ± standard error of the mean (SE). For the statistical analysis of the obtained data sets and the determination of the level of significance, a one-way analysis of variance (ANOVA) with Tukey's post hoc test was conducted. The differences between the obtained values were considered significant at $P < 0.001$, 0.01 and 0.05.

3. Results and discussion

3.1. Initial droplet characterization

The present study aimed to introduce phospholipids as natural, food-grade surfactants and to utilize low-energy approaches to develop edible NEs with promising clinical and therapeutic applications. Three combinations of soy phospholipid mixture and the co-surfactant Tween 20 were used to fabricate NEA, NEB, and NEC, with other process parameters held constant. A bluish tinge was observed on the surface of the formulation, indicating the presence of nano-droplets (Fig. 1a) with no flocculation tendency in the three NE formulations, suggesting that all were homogeneous and highly stable. We studied the changes in the NEs after centrifugation at 8000 rpm for 10 min. Although a creaming effect was observed, no prominent phase separation occurred after centrifugation, indicating satisfactory stability of the formulations (Fig. 1b). The findings in our study corroborate the perception of good kinetic stability in the NE system, comprising tiny oil droplets.

The initial droplet size distributions of the fabricated formulations stabilized withasolectin and Tween-20 are shown in Table 1. Droplets of NEs for all the formulations, NEA, NEB, and NEC, depicted an initial hydrodynamic diameter of approximately 60–90 nm with a narrow monomodal distribution. The electrical charge on the surface of the oil droplet in the NE was quantified by measuring the formulation's zeta potential. The highly negative zeta potential of the formulations NEA, NEB and NEC might contribute to the strong electrostatic repulsion among the emulsified lipid droplets in the continuous aqueous medium, stemming from the interfacial localisation of anionic phospholipids on the oil droplets, thereby leading to good stability. The anionic soy

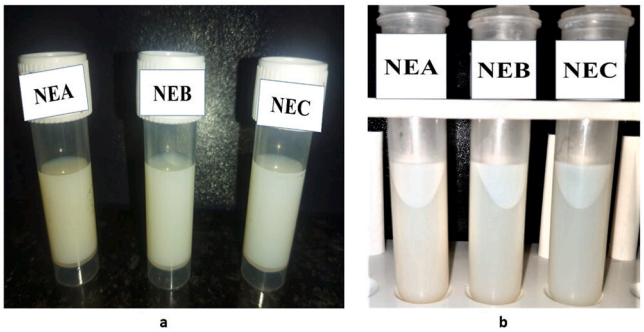


Fig. 1. Visual observation of the freshly prepared nanoemulsions, e.g., NEA, NEB and NEC.

phospholipids stabilized the NEs, and the high negative zeta potential observed is a direct consequence of their adsorption onto the droplet surface. Phosphatidylserine and phosphatidylinositol carry negatively charged head-groups at physiological pH, which confer a net negative charge to the surface of the dispersed lipid droplets. This surface charge gives rise to a strong electrostatic repulsion between individual oil droplets suspended in the continuous aqueous phase. The electrostatic repulsion arising from the high zeta potential plays a crucial role in preventing droplet aggregation, thereby enhancing the kinetic stability of the NE. Importantly, the zeta potential is the cause of the electrostatic stabilization. A high zeta potential (typically $> \pm 30$ mV) indicates that repulsive forces dominate van der Waals attraction, reducing the likelihood of coalescence or flocculation [21]. TEM images revealed that the spherical droplets in all three formulations were uniformly dispersed in the field (Fig. 2). In the present study, no significant difference was observed among the three formulations.

3.2. Influence of primary emulsification- high-speed homogenization and solvent evaporation approach on nanoemulsion fabrication

By replacing established high-energy techniques with a hybrid homogenization-evaporation approach, the present study introduced a novel technology that combines high-speed homogenization and solvent evaporation to develop food-grade NEs in an energy-efficient, cost-effective manner.

Primary emulsification under magnetic stirring: Ethyl acetate, an amphiphilic, volatile organic solvent with FDA-approved GRAS status, was mixed with the oil to form the dispersed phase. Ethyl acetate has moderate water solubility (8% w/v under ambient conditions). During the initial low-speed magnetic stirring for 2 h, a portion of the ethyl acetate spontaneously diffuses into the continuous aqueous matrix. This mass transfer establishes a stable partition coefficient between the continuous and dispersed domains and initiates an intrinsic spontaneous shrinkage effect before high-speed shearing begins [7].

High-speed homogenization: During homogenization, droplet size reduction is governed by the competition between droplet disruption (driven by hydrodynamic shear and turbulent flow) and droplet re-coalescence (driven by Brownian collisions) [22]. The oil droplets were found to decrease in size due to turbulent flow and hydrodynamic shear stress generated within the instrument as the stirring speed increased. In addition to stirring speed, process time was found to be effective in reducing droplet size and polydispersity index. The disruption of oil droplets had already been reported to be enhanced with reduced viscosity of the dispersed phase [23]. Pure sesame oil has a high bulk viscosity of 36.5 mPa · s. Fluid dynamics dictate that droplet disruption in a shear field is highly efficient when the viscosity ratio between the dispersed phase (ηD) and the continuous phase (ηC) approaches parity ($0.05 < \eta D/\eta C < 5$) [24]. Ethyl acetate features an exceptionally low viscosity (0.455 mPa · s at 25°C). Diluting the oil core with ethyl acetate lowers the viscosity of the organic phase, allowing the mechanical energy from the rotor-stator mixer to easily break down the droplets. The size of the oil droplets generated by high-speed homogenization was also found to be curtailed with decreasing interfacial tension [25]. In the present study, the interfacial tension (γ) at the sesame oil/water interface was 17mN m^{-1}. In contrast, at the oil-ethyl acetate/water interface, the interfacial tension was only 6.8 mN m^{-1} at ambient temperature (Fig. 3a). This dramatic reduction in viscosity and interfacial tension in the presence of ethyl acetate significantly lowers the Critical Capillary Number (Ca_{crit}) required for droplet rupture [26], thereby enabling standard mechanical high-speed homogenization (10, 000 rpm) to achieve nanometric fragmentation. High-speed homogenization for more than 45 min might cause re-coalescence of droplets, a subsequent increase in droplet size, undesirable lipid oxidation, thermal degradation of phospholipid and Tween 20 [27].

Solvent evaporation: Solvent evaporation is widely used in the preparation of self-emulsifying nanodelivery systems [28]. Ethyl acetate possesses a low boiling point of 77.1°C under atmospheric pressure. It can be easily removed from the system under reduced pressure to achieve the final droplet size and ensure homogeneous distribution [7]. The effect was attributed to the shrinkage of the emulsified droplets as the volatile solvent is expelled [29,30].

Based on our study, ethyl acetate was identified as the most crucial factor for achieving a significant reduction in NE droplet size during primary emulsification, high-speed homogenization, and the final solvent evaporation step.

3.3. Influence of mixed emulsifier on nanoemulsion formulation

Although natural phospholipids have been widely used as classical emulsifiers for years, a phospholipid mixture is preferred over lecithin alone in most NE fabrication [31]. Lecithin alone has been previously reported to impart an inadequate electrical charge to the droplet surface. Hence, electrostatic stabilization between lecithin-coated emulsified lipid droplets proved insufficient and eventually led to coalescence, thereby hindering long-term stability. On the contrary, emulsions stabilized with mixtures of phospholipids possessing sufficiently high surface charge were reported to exhibit a noticeable increase in resistance against flocculation due to the electrostatic repulsion between the emulsified oil droplets. The highly negative zeta potential of the formulations depicted in our study (Table 1) agreed with the previous literature showing that the surface electrical charge of the droplets in phospholipid-based NE was usually found in the negative range due to the presence of negatively charged phospholipids, as well as free fatty acids and phosphatidic acid in the system [32]. In our study, we have employed asolectin as an emulsifier. Asolectin is a heterogeneous mixture of phospholipids, consisting of 25% phosphatidylcholine (PC), 25% phosphatidylethanolamine (PE) and 25% phosphatidylinositol (PI) along with a minute quantity of other phospholipids and polar lipids [33]. PC and PE are uncharged at physiological pH (7.4), but PI and smaller quantities of acidic lipids, such as phosphatidylserine and

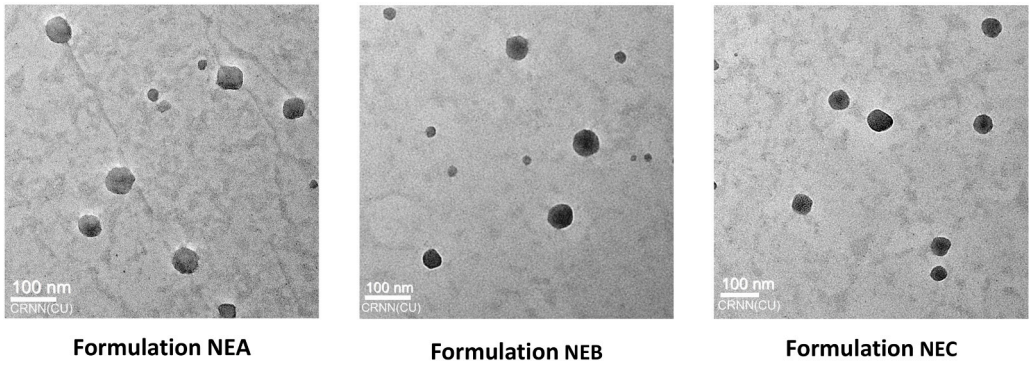


Fig. 2. Size, shape and droplet distribution of the fabricated nanoemulsions NEA, NEB, and NEC as visualised by Transmission electron micrographs. (scale: 100 nm).

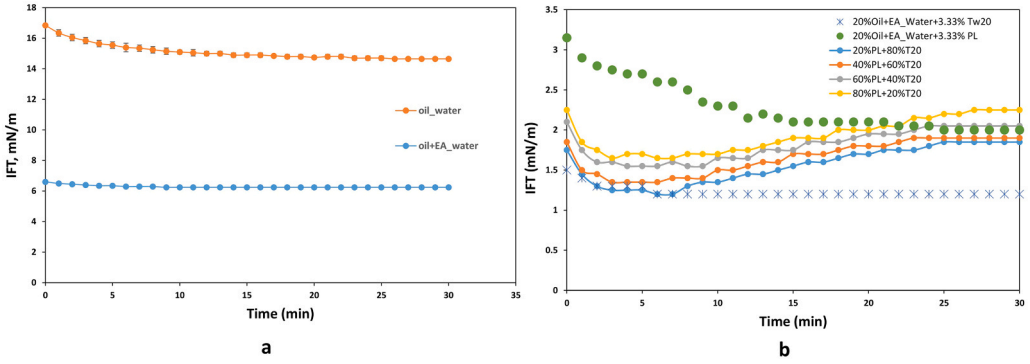


Fig. 3. Interfacial tension at the oil-water interface of the system in the presence of ethyl acetate(Fig. 3**a**); Influence of emulsifier and co-emulsifier on the interfacial tension; the interfacial tension reduced by the mixed emulsifier system such as- 20% phospholipid + 80% Tween 20, 20% phospholipid + 80% Tween 20, 20% phospholipid + 80% Tween 20, 20% phospholipid + 80% Tween 20 finally resembled the interfacial tension reduced by phospholipid alone indicating the dominance of phospholipid (PL) over Tween 20 at the interface **(**Fig. 3**b)**.

phosphatidylglycerol, are ionized at pH 7.0. Thus, they imparted a highly negative charge to the interface between emulsion droplets and influenced the surface electrical characteristics, favouring electrostatic stabilization. In addition to charge-induced stabilization, various studies have demonstrated that phospholipid mixtures improve molecular packing at the interface [31]. The distinct hydration behaviour of differently charged phospholipid head groups was shown to lead to different molecular head-group space requirements and packing behaviour at the interface. According to previous reports, the presence of PI and PE enhanced the swelling of the lamellar liquid-crystalline phase of PC, thereby stabilizing O/W emulsions [34]. To fabricate a stable NE formulation, our study has explored asolectin as an emulsifier, owing to its PE and PI content, which are present at percentages similar to those of PC. Furthermore, Tween 20 was introduced in our study to interact with asolectin, modifying the dimensionless packing parameter and achieving steric stabilization [35]. The addition of surface-active, hydrophilic stabilizing agents has been reported to reduce packing parameters, thereby making the interfacial film more flexible and accommodating the curvature of emulsified nanodroplets [36]. In theory, a salient parameter for characterizing the surfactant film is the spontaneous mean curvature, H_0, which quantifies the monolayer's inherent tendency to bend away from a flat geometry [37]. A high H_0 promotes the formation of flexible interfacial films, whereas a low H_0 promotes the formation of a more rigid layer. The value of H_0 was positive for hydrophilic surfactants, such as Tweens, owing to their bulky headgroups and pliable hydrocarbon moieties [38]. Furthermore, the presence of lecithin alone was not supposed to favour emulsion stability in different environmental conditions; therefore, to achieve the desired emulsion stability, a combination of natural phospholipids or the use of a mixed emulsifier system was found to be suitable [39]. In our study, incorporating hydrophilic surfactants, such as Tween 20, as co-emulsifiers alongside a phospholipid mixture in an O/W NE formulation helps achieve a more balanced hydrophilic-lipophilic balance (HLB) in the interfacial layer. Phospholipids, being amphiphilic, often provide structural rigidity at the oil–water interface, while Tween 20, with a high HLB value (~16.7), enhances the hydrophilicity of the interfacial film. This co-surfactant promotes greater interfacial film flexibility, thereby reducing interfacial tension and facilitating the formation of smaller, more stable oil droplets. Additionally, the mixed surfactant system supports a favourable spontaneous curvature toward the aqueous phase, which is critical for stabilizing oil droplets in the continuous aqueous medium of biphasic emulsions. Mechanistically, Tween 20 intercalates between phospholipid molecules at the droplet interface, disrupting rigid packing and allowing for dynamic rearrangement of the surfactant layer. This enhances droplet deformability, promotes efficient packing geometry, and minimises Laplace pressure, thereby stabilizing the NE and improving its physical properties.

Interestingly, in our experimental design, no significant differences were observed among the formulations in size and charge; however, formulation NEA exhibited a slightly more negative zeta potential than the other formulations. This might be attributed to the quantity of phospholipid mixture and Tween 20 present in the system, and thus their structural rearrangements at the interfacial layer surrounding the lipid droplets. Formulation NEA and formulation NEC contained maximum and minimum amounts of asolectin, respectively. In our study, the interfacial tension profiles of asolectin, Tween 20, and a blend of asolectin and Tween 20 in different ratios are demonstrated in Fig. 3b. It was observed that asolectin and Tween 20 presented the highest and lowest interfacial tension values, respectively. The observed differences in interfacial tension between asolectin and Tween 20, when tested individually, can be attributed to their molecular weights and interfacial adsorption behaviours. Asolectin (~0.76 kDa), a complex mixture of phospholipids, exhibited a higher interfacial tension than Tween 20 (~1.23 kDa), a nonionic surfactant known for its strong surface activity. This counterintuitive result arises from the influence of molecular size on translational entropy. At lower molecular weights, such as that of asolectin, molecules possess higher translational mobility in the bulk aqueous phase. This enhanced entropy discourages sustained adsorption at the oil–water interface, as the entropic cost of localising small, mobile molecules at an interface is relatively high. As a result, asolectin displays weaker interfacial accumulation, reducing its effectiveness in lowering interfacial tension. In contrast, Tween 20, with a slightly higher molecular weight and more flexible polyoxyethylene chains, experiences reduced entropic penalties upon adsorption. Its amphiphilic structure enables rapid, dense adsorption at the interface, thereby lowering interfacial tension by displacing water molecules and reducing cohesive forces at the oil–water boundary [40]. In our study, the most interesting interfacial tension profile was demonstrated for the combination of asolectin and Tween 20 in different ratios. Initially, the interfacial tension of a mixture of asolectin and Tween 20 was lower and similar to that imparted by Tween 20 alone. However, over time, the interfacial tension of the emulsifier mixture gradually increased and eventually became comparable to that of asolectin alone. Based on the above findings, it can be hypothesised that Tween-20 molecules with a high HLB value primarily reduce the interfacial tension of the system by adsorbing more quickly at the oil-water interface than asolectin [41]. Subsequently, the soy-phospholipid mixture replaced Tween-20 at the interface. It formed a multi-lamellar viscoelastic layer around the lipid droplet, likely due to the self-assembly of phospholipids at the interface. In our study, the interfacial behaviour of the formulations was expected to be dominated by asolectin, with Tween 20 as a co-emulsifier. Asolectin, due to its amphiphilic phospholipid structure, preferentially adsorbs at the oil–water interface, forming a rigid, stabilizing monolayer around oil droplets through its hydrophobic acyl chains (anchored in oil) and

hydrophilic head groups (exposed to the aqueous phase). Tween 20 intercalates into the phospholipid monolayer, disrupting the tight molecular packing of asolectin and introducing interfacial flexibility. This synergistic interaction reduces the overall interfacial tension more effectively than either emulsifier alone [42]. Tween 20 likely occupies interfacial spaces between asolectin molecules, thereby optimizing curvature and enabling a more homogeneous, fluid interfacial film. Thus, while asolectin structurally dominates the interface, the co-adsorption of Tween 20 enhances interfacial dynamics, promoting emulsification efficiency and droplet stability. The hypothesis was supported by measuring the surface electrical charge of the droplets (Table 1). The highest magnitude of negative zeta potential, indicating strong electrostatic repulsion, was obtained for the formulation NEA, which might be attributed to the presence of a substantial amount of asolectin, an anionic surfactant. Similarly, a relatively lower negative zeta potential was observed for the formulation NEC, probably owing to the higher amount of the non-ionic emulsifier Tween 20 compared to asolectin. Furthermore, the enhanced stability of NE produced by solvent evaporation upon the addition of Tween or Span-type small--molecule surfactants to lecithin can be attributed to interfacial tension modulation and interfacial film optimization. Lecithin adsorbs at the oil–water interface, forming a structurally rigid monolayer. However, lecithin alone may not sufficiently reduce interfacial tension, particularly in dynamic or kinetically unstable systems. When small-molecule surfactants, such as Tween (hydrophilic) or Span (lipophilic), are co-introduced, they rapidly adsorb at the interface, displacing water molecules and packing efficiently alongside lecithin. This co-adsorption leads to a greater reduction in interfacial tension, which is a thermodynamically favourable condition that facilitates the formation of smaller oil droplets during emulsification and reduces the Laplace pressure that drives coalescence [43]. Furthermore, the small surfactants enhance interfacial film flexibility and mobility, enabling the interfacial layer to better adapt to curvature changes and dynamic stresses during droplet formation and storage. Lecithin provides structural integrity and anchoring at the interface, while Tween/Span molecules enhance interfacial packing, lower interfacial energy, and contribute to steric and/or electrostatic repulsion between droplets. This combination effectively prevents droplet coalescence, aggregation, and Ostwald ripening, thereby enhancing the kinetic and thermodynamic stability of NEs [31].

3.4. Shelf-life stability analysis

In the present work, the variation in hydrodynamic diameter and zeta potential of the three fabricated nano-formulations was thoroughly studied over an 8-week storage period to gain insight into their overall stability. In the final week, formulations NEA, NEB, and NEC showed increases in size of approximately 59%, 80.7%, and 132%, respectively, relative to the initial one, as depicted in Fig. 4a. Though the initial (at 0 weeks) diameter of formulation NEA, comprising the highest percentage of asolectin was found to be higher than formulation NEB and NEC by about 8.33% and 11.96% respectively, (the difference was not statistically significant), formulation NEA provided maximum resistance to droplet aggregation and instability of the system as evinced from the final droplet size analysis; illustrated in Fig. 4b. On the contrary, initially, formulation NEC was found to have smaller droplets than

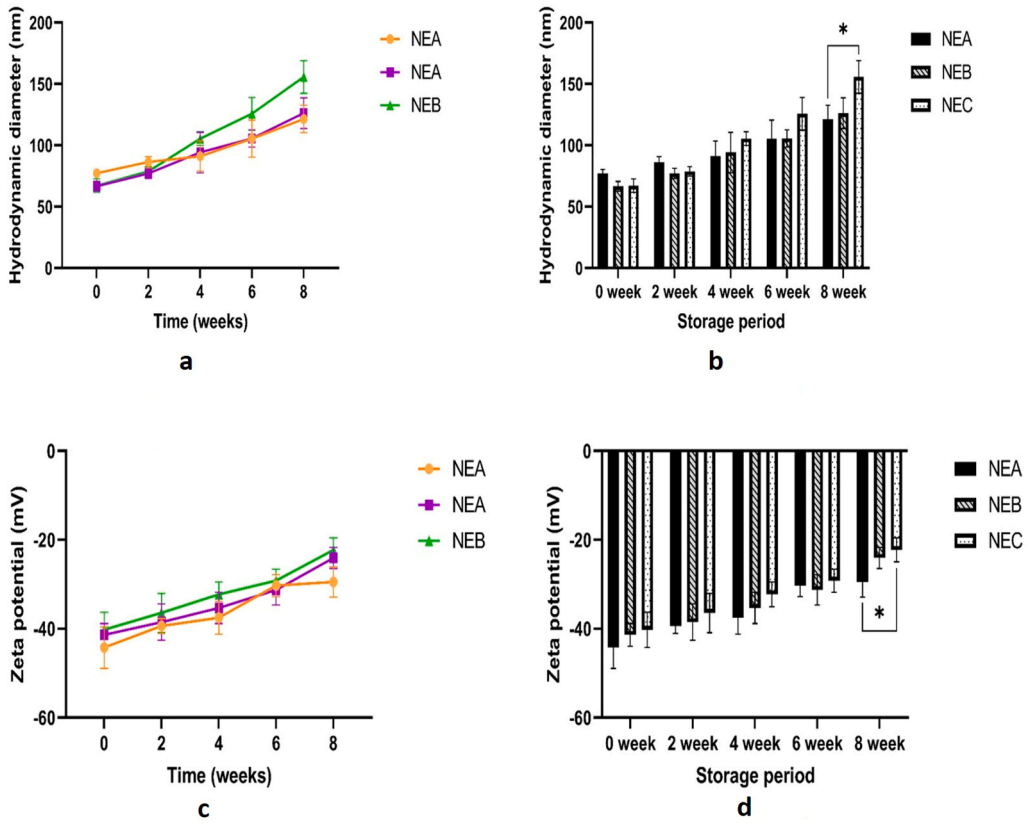


Fig. 4. Evaluation of shelf-life stability of nanoemulsion formulations NEA, NEB and NEC in terms of hydrodynamic diameter **(**Figs. 4**a and** 4**b)** and in terms of zeta potential (Figs. 4**c and** 4**d)** during storage at 25℃ temperature. The ascending trend in droplet diameter of NEA, NEB, and NEC between the initial and final weeks of storage is depicted in Fig. 4**a**. The comparative analysis of droplet diameters for NEA, NEB, and NEC across different storage time intervals is shown in Fig. 4**b**. The decreasing trend in the zeta potential values of NEA, NEB, and NEC from the initial to the final week of storage is shown in Fig. 4**c**. The comparative analysis of the zeta potentials of NEA, NEB, and NEC at different time points during storage is shown in Fig. 4**d**. Results were represented as Mean ± SD (n = 3); '*' suggested a significant difference at the $p < 0.05$ level.

formulations NEA and NEB; however, in the final estimation, formulation NEC showed droplet diameters that were about 22% and 18.85% higher than those of formulations NEA and NEB, respectively (Fig. 4b). Notably, in the final week, the droplet diameter of NEC was found to be significantly ($p < 0.05$) higher than that of formulation NEA.

In the case of zeta potential analysis, the formulations exhibited a tendency similar to that of size. During storage, the zeta potential decreased by only about 32.6% for the NEA formulation. In comparison, the decreases in NEB and NEC were nearly identical, at 43% and 44.5%, respectively, as depicted in Fig. 4c. Furthermore, at the initial period (0 weeks), the difference in zeta potential among the three formulations was not statistically significant at all. However, in the final week, after continuous loss of surface charge, formulation NEC was shown to have a significantly lower zeta potential ($p < 0.05$) than formulation NEA (Fig. 4d). Mean and standard deviation are calculated from three observations in each group (Figs. 4a, 4b, 4c, 4d).

During storage at 25℃, the non-ionic polyoxyethylene head groups of Tween 20 undergo subtle thermal dehydration, altering the optimum curvature of the surfactant monolayer at the interface [29]. Being a non-ionic surfactant, Tween 20 cannot form a strongly cross-linked network with adjacent molecules; it is prone to interfacial deformation during thermal motion. This enables localized droplet flocculation and subsequent coalescence, increasing the average droplet size from an initial 67.12 nm to approximately 155 nm in NEC, which had the highest Tween 20 concentration. At this sub-micron scale, the forward kinetic velocity driven by gravitational buoyancy (v) is still small enough to be completely counteracted by Brownian motion and thermal diffusion. Consequently, while the internal droplet architecture undergoes coalescence, the bulk system resists macro-creaming or phase separation under ambient gravity. The substantial decrease in zeta potential in formulations NEB and NEC may be attributed to the presence of flocculated droplets. Furthermore, strong resistance to interfacial deformation was observed in the NEA formulation, which contained the highest amount of asolectin. According to previous literature, the current findings may be attributed to the formation of a two-dimensional viscoelastic layer, strengthened by the self-assembly of phospholipid molecules and by hydrogen bonding among the phosphate groups of neighbouring phospholipid molecules [44]. Based on the above findings, a perfect blend of asolectin and Tween 20 was suggested to achieve the intended stability of the NE formulation.

3.5. *Effect of pH in the fabricated nanoemulsion system*

The impact of varying pH on the storage stability of three different formulations was assessed through average droplet size analysis. In the current research, across the pH range of 6–8, all three formulations (NEA, NEB, and NEC) exhibited excellent stability, with no significant variation in droplet size, as revealed by particle-size analysis. At pH 4, particle-size analysis showed a notable increase in the average droplet diameter across all formulations, indicating a tendency towards physical destabilization (Fig. 5a). Compared with the droplet diameter at neutral pH, formulations NEA, NEB, and NEC showed increases of 332.8%, 153%, and 141.7%, respectively, at pH 3, as depicted in Fig. 5a. Although all three formulations underwent substantial changes in

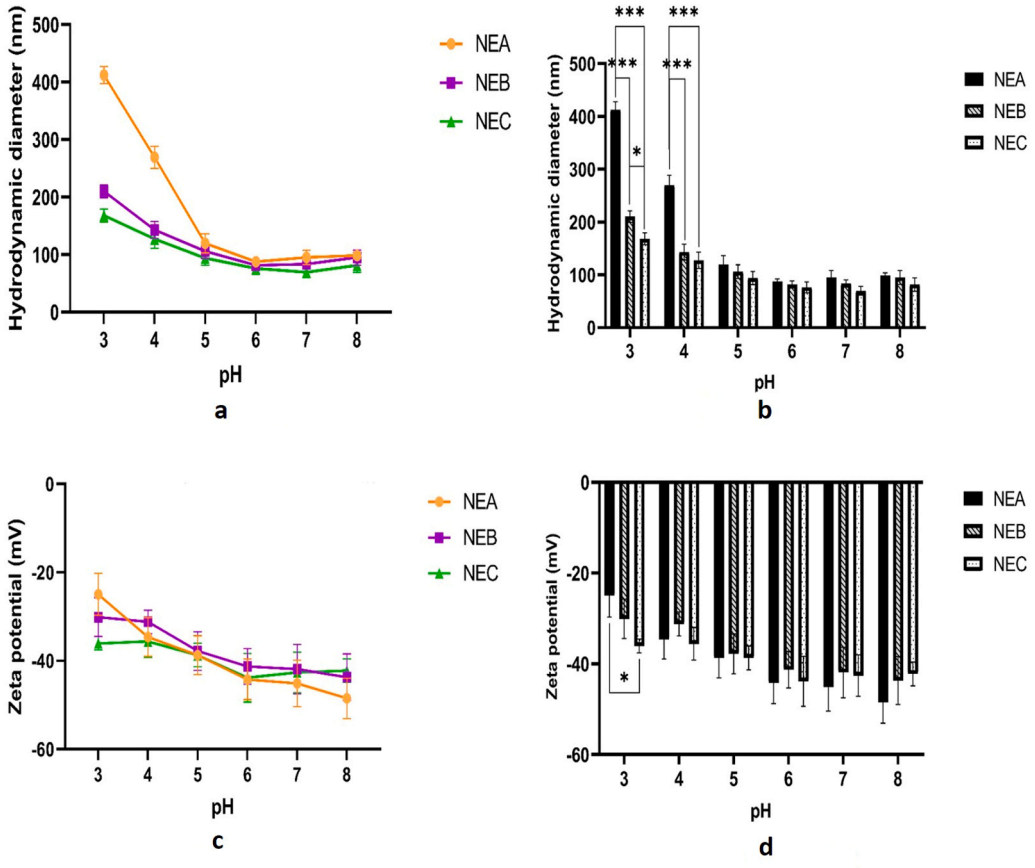


Fig. 5. Evaluation of shelf-life stability of nanoemulsion formulations NEA, NEB and NEC in terms of hydrodynamic diameter (Figs. 5**a and** 5**b)** and zeta potential (Figs. 5**c and** 5**d)** in a broad range of pH (pH 3–8). The ascending trend in the hydrodynamic diameters of NEA, NEB, and NEC in the acidic pH medium was depicted in Fig. 5a; the comparative analysis of their hydrodynamic diameters across different pH values was shown in Fig. 5**b**. The descending trend of zeta potential values for NEA, NEB, and NEC in the acidic pH medium is depicted in Fig. 5**c**. A comparative analysis of the zeta potential values for NEA, NEB, and NEC at different pH values is shown in Fig. 5**d**. Results were stated as Mean ± SD (n = 3); '*' suggested a significant difference at $p < 0.05$ level; '***' suggested a significant difference at $p < 0.001$ level.

droplet diameter at acidic pH, the effect was greatest in formulation NEA, which had a higher asolectin content than the others. At pH 3, the increase in droplet diameter was significantly higher ($p < 0.001$) in formulation NEA compared to NEB and NEC, as depicted in Fig. 5b. Furthermore, at acidic pH, the droplet diameters of formulations NEB and NEC were significantly different at the $p < 0.05$ level.

To explain this physical destabilization, the zeta potentials of the formulations at different pH levels were measured in detail. A considerable reduction in surface potential, from highly negative values at neutral and basic pH to weakly negative values at acidic pH, was observed for all three formulations (Fig. 5c). At pH 3, the zeta potential of formulation NEA was shown to decrease by 37.02% from the values at neutral pH, while that of NEB and NEC decreased by 28.16% and 21.6%, respectively, as depicted in Fig. 5c. Most importantly, a significant ($p < 0.05$) decline in zeta potential values was perceived in the formulation NEA compared to NEC at pH 3 (Fig. 5d). Mean and standard deviation are calculated from three observations in each group (Figs. 5a, 5b, 5c, 5d).

3.6. *Effect of ionic strength in the fabricated nanoemulsion system*

Upon a substantial increase in salt concentration (>200 mM) in the system, particle-size analysis revealed a gradual increase in the mean hydrodynamic diameter of the droplets, indicating flocculation. At 500 mM salt concentration, the droplet diameter of formulation NEC was increased by 176.77% while that for NEA and NEB was by 238.85% and 184.32%, respectively (Fig. 6a). Furthermore, at high ionic concentrations (400 and 500 mM), formulation NEA exhibited a notable increase in droplet diameter compared to NEB and NEC, with $p < 0.05$ and $p < 0.01$, respectively (Fig. 6b). According to the previous report, as the ionic strength of the medium increased, a concomitant decrease in the electrostatic repulsion between the droplets was observed, suggesting the accumulation of counterions around the emulsified droplet [45]. Excessive salt concentration in the system could nullify the surface charge of the emulsified droplet, possibly due to electrostatic screening. In addition to screening negative charges, positively charged ions in the medium can form bridges between adsorbed phospholipids on the droplets. The salt ions in the aqueous medium electrostatically screen the negative surface charges on the emulsified droplets, thereby reducing the zeta potential and weakening the electrostatic repulsion that prevents droplet aggregation. As a result, the droplets are more likely to come into proximity, and ions can form ionic bridges between adjacent negatively charged phosphate head groups of phospholipid molecules adsorbed at the droplet interfaces [46]. This bridging effect further reduces interfacial repulsion and promotes inter-droplet attraction, destabilizing the NE. Sodium ions (Na^+), due to their single positive charge and high hydration energy, primarily remain solvated and do not effectively displace water molecules to bridge between adjacent phospholipid head groups, as they lack sufficient charge density to induce bridging interactions. As a result, they cannot form stable ion bridges like divalent or trivalent cations can. Furthermore, above a critical salt level, salt ions were found to adsorb a fraction of water molecules [47]. Hence, the number of water molecules interacting with the emulsifier's charged group was markedly reduced. As a result, the repulsive force between the polar groups of phospholipids was found to decrease, and the hydrophilic head groups started to unite in the centre, causing the emulsified lipid droplets to flocculate. On the contrary, at a small salt concentration of the medium, the electrostatic repulsion was found to be

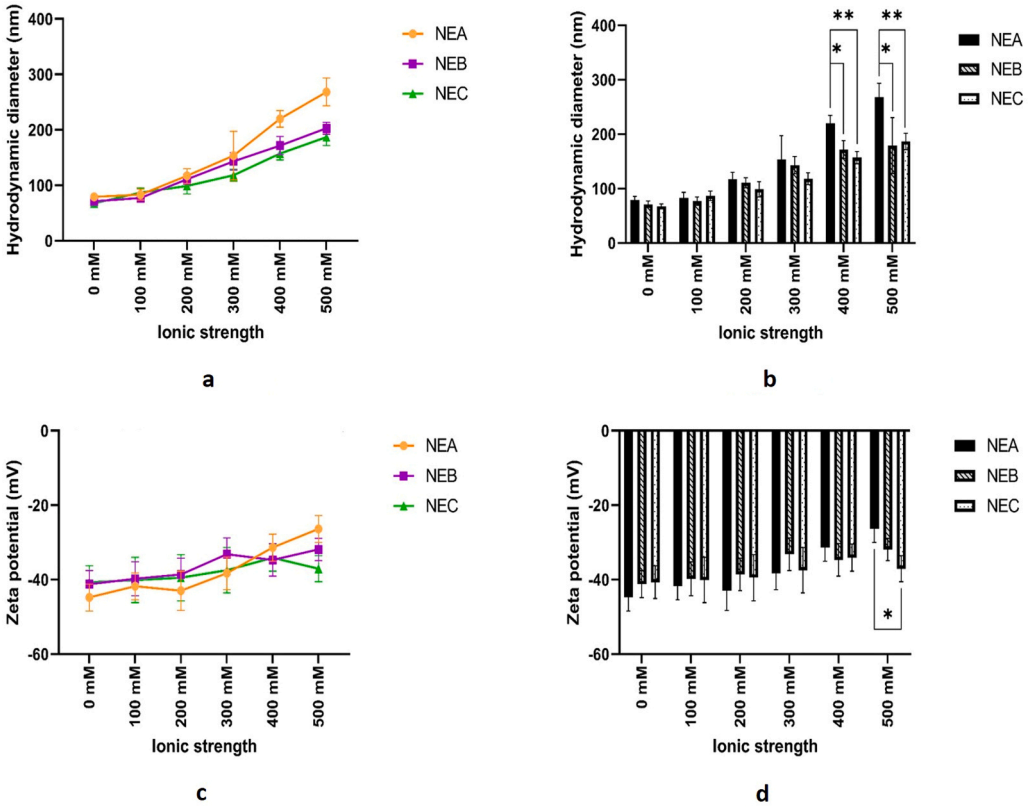


Fig. 6. Evaluation of shelf-life stability of nanoemulsion formulations NEA, NEB and NEC in terms of hydrodynamic droplet diameter **(**Figs. 6**a and** 6**b)** and zeta potential **(**Figs. 6**c and** 6**d)** in a varied range of ionic strength (0–500 mM). The ascending trend in the hydrodynamic droplet diameter of NEA, NEB, and NEC at higher ionic strength is depicted in Fig. 6**a**. The comparative analysis of the hydrodynamic droplet diameter among NEA, NEB, and NEC at varying ionic concentrations is shown in Fig. 6**b**. The descending trend of the zeta potential of NEA, NEB, and NEC at higher ionic strengths is depicted in Fig. 6**c**. A comparative analysis of the zeta potential among NEA, NEB, and NEC in varying ionic concentrations is shown in Fig. 6**d**. Results were stated as Mean ± SD (n = 3); '*' suggested a significant difference at $p < 0.05$ level; '**' suggested a significant difference at $p < 0.01$ level.

sufficient to surpass the attractive van der Waals forces and hydrophobic interactions.

In the present study, a considerable decline in zeta potential was observed, from highly negative values (without salt) to weakly negative values (with 500 mM salt in the medium) across all formulations (Fig. 6c), which may be attributed to electrostatic screening. Though all three formulations followed an ascending trend in droplet size and a descending trend in zeta potential with increasing the ionic strength of the solution, the surface potential of formulation NEC was shown to decrease by 13% while that of NEA and NEB by 38.83% and 22.69% respectively in 500 mM ionic concentration compared to the initial one (Fig. 6c). Furthermore, the zeta potential has been significantly reduced ($p < 0.05$) in the NEA formulation compared to NEC at a salt concentration of 500 mM (Fig. 6d). Mean and standard deviation are calculated from three observations in each group (Figs. 6a, 6b, 6c, 6d).

Increasing NaCl concentration introduces sodium ions (Na^+) into the aqueous phase, which screen the negative surface charges on the oil droplets by accumulating in the electrical double layer surrounding each droplet. This leads to compression of the double layer and a reduction in the zeta potential, weakening the electrostatic repulsion that usually prevents droplet–droplet interactions. As the zeta potential approaches zero, repulsive forces are no longer sufficient to avoid droplet aggregation. The oil droplets begin to flocculate or coalesce, increasing their hydrodynamic diameter. With a higher increase in NaCl concentration, a higher ionic strength more effectively suppresses repulsive barriers and promotes van der Waals attractions between droplets.

Previous literature has shown that NEs stabilized with Tween-type nonionic surfactants are sufficiently resistant to electrostatic destabilization and droplet aggregation owing to steric stabilization [48]. Thus, the Formulation NEA, containing a minimum percentage of Tween 20, was found to be more vulnerable to a strong ionic environment, while formulation NEC, possessing the highest percentage of Tween 20, exhibited intended stability in varying ionic strength owing to this steric hindrance. Its hydrated polyethene oxide chains form a dense, brush-like barrier around the oil droplets. When droplets approach each other, these flexible chains overlap and compress, increasing osmotic pressure and decreasing the system's entropy.

3.7. Lipid oxidation study: impact of phospholipid content in the fabricated nanoemulsion

The baseline TBARS level of approximately 0.2 nmol/mL was observed in freshly prepared NEA, NEB, and NEC stems due to the raw material composition and processing methods. Commercial-grade unpurified phospholipid mixtures, such as asolectin, are highly complex matrices rich in polyunsaturated fatty acids (PUFAs), such as linoleic and linolenic acids. These polar lipid structures are intrinsically prone to trace-level autoxidation during primary extraction, industrial packaging, and long-term storage before procurement. Furthermore, negatively charged emulsifiers, such as phospholipid, will attract positively charged transition-metal ions, thereby stimulating the formation and decomposition of lipid hydroperoxides [49,50]. The mechanical energy during high-speed homogenization introduces dissolved atmospheric oxygen into the water-solvent continuum, accelerating radical generation and causing a minor level of localized processing autoxidation. In traditional lipid oxidation kinetics, an elevated primary peroxide baseline catalyses the onset of an exponential propagation phase. However, our 8-week monitoring data reveals a stable, controlled linear increase rather than a catastrophic exponential spike across all three matrices (NEA, NEB, and NEC). Mean and standard deviation are calculated from three observations in each group, and the total amount of TBARS generated in the formulations at the final week of storage was found as follows: formulation NEC> formulation NEB> formulation NEA (Fig. 7). In the present work, formulation NEC exhibited maximum oxidation of emulsified lipids significantly higher than formulation NEA and NEB at $p < 0.001$ and $p < 0.05$ levels. Additionally, a significant

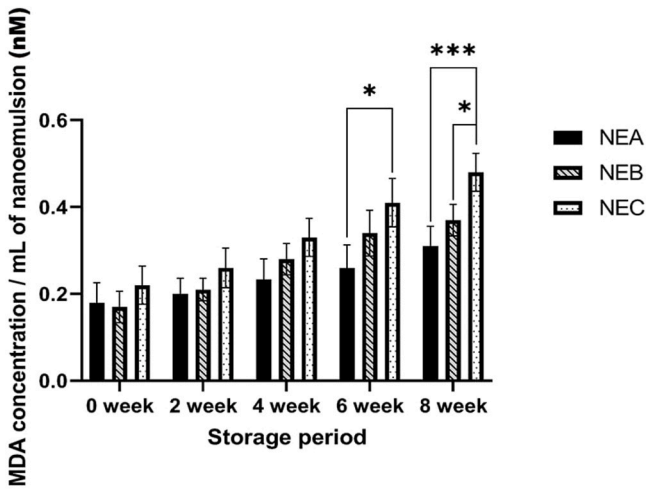


Fig. 7. Comparative analysis on oxidative stability of the formulated nanoemulsions NEA, NEB, and NEC at 25℃ during the storage period of 8 weeks; Results were stated as Mean ± SD. '*' suggested a significant difference at $p < 0.05$ level; '***' suggested a significant difference at $p < 0.001$ level.

difference ($p < 0.05$) was observed between the TBARS concentrations of NEA and NEC at the 6th week of storage.

In the present study, the percentage of asolectin was found to be crucial in determining the level of lipid oxidation in the fabricated NEs. Asolectin molecules preferentially pack at the oil-water interface, forming a thick, viscoelastic multi-lamellar framework around the core sesame oil drops. This structure mitigates radical propagation by physically shielding the inner core from water-soluble pro-oxidants and transition metals. Since NEC is dominated by the small-molecule synthetic surfactant Tween 20, it lacks a tightly packed, cross-linked phospholipid network. This structural gap leaves the matrix vulnerable to peroxyl radical propagation [51]. Hydroperoxide formation was significantly higher in Tween-20-stabilized nanoemulsion compared to phospholipid-stabilized nanoemulsion [50]. On the contrary, lecithin regenerates major antioxidants such as tocopherols [52]. Phospholipid may also accelerate antioxidative activity by forming non-enzymatic browning reaction products through interactions with lipid oxidation products. It may chelate prooxidative transition metals, thereby mitigating lipid peroxidation [53].

3.8. Free fatty acid release study: influence of interfacial composition on lipolysis

Sesame is a rich source of bioactive compounds. It exhibits a wide range of bioactivities in physiological systems [54]. As the fabricated formulations are intended to serve as delivery vehicles for therapeutic lignans, it is necessary to assess their digestibility under *in vitro* conditions that simulate the human gastrointestinal tract. In the simulated mouth and gastric phase, no distinguishable difference in free fatty acid release was observed among the three formulations NEA, NEB and NEC. There was no lag phase; the initial rate of free fatty acid release during the first 15 min was rapidly augmented for all three formulations (Fig. 8). Lipid digestion occurred predominantly within the simulated small-intestinal phase. Over time, the NEA formulation was digested more than NEB and NEC. At 30–45 min, formulation NEB and NEC showed free fatty acid release around 22–23%, while about 26% was observed for the formulation NEA. Throughout the digestion period, the release of fatty acids from the formulation NEA increased linearly; however, for formulations NEB and NEC, the trend was nonlinear, showing saturation at the end of digestion. Formulation NEA exhibited maximum release of free fatty acid (72.65%).

Previous observations demonstrated that lipolysis was enhanced in

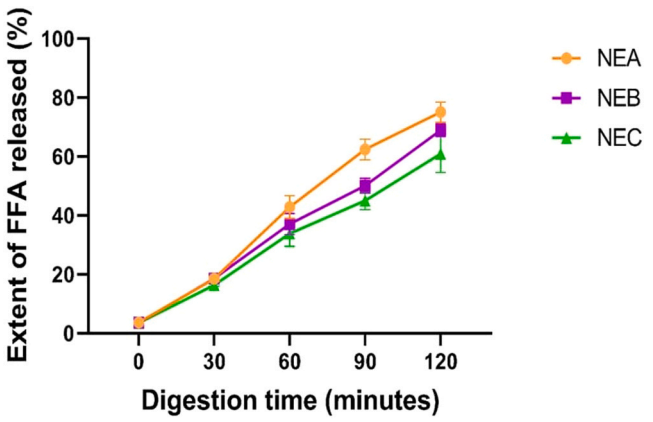


Fig. 8. Free fatty acid release kinetics of the nano formulations NEA, NEB, and NEC in the simulated intestinal phase; results were stated as Mean ± SD (n = 3).

the presence of a phospholipid emulsifier compared to Tween 20 in the absence of bile extract [55]. However, in the presence of bile salts, the current study indicated markedly higher rates and extents of free fatty acid generation during the simulated intestinal phase in the NEA formulation (1.2 w/w % asolectin). The calcium ions and bile salts present in the intestinal medium have been reported to displace emulsifier mixtures and long-chain fatty acids that accumulate at the droplet surface, thereby facilitating pancreatic lipase access to the interface [56,57]. During intestinal digestion, a higher zeta potential in NEA can render the droplet interface more favourable for bile salt adsorption [18,58]. Recent reports have shown that using phospholipids as emulsifiers or adding them under simulated intestinal conditions increases the rate and extent of lipid digestibility in emulsion systems [59]. The presence of bile salts in the intestinal condition was found to promote the destruction of a well-packed phospholipid interface, resulting in a mixed phospholipid/bile salt interface [60]. This mixed interface induces transient structural packing defects and increases overall interfacial fluidity. These transient packing defects would promote substantial binding of the pancreatic lipase-co lipase complex to the oil-water interface, as well as enzymatic action on the emulsified oil droplets [61]. A critical block during the intestinal digestion of long-chain triglycerides (such as those in sesame oil) is the accumulation of lipolysis products (free fatty acids and monoglycerides) at the droplet surface. In practice, FFA accumulated around the droplet was reported to restrict lipase access to the droplet surface and hinder lipolysis [62,63]. During the initial phase of lipolysis, digested free fatty acids have also been reported to facilitate the formation of mixed micelles, with assistance from surface-active soy phospholipids and bile salts present in the medium [64]. In the presence of Ca^{2+}, the mixed micelle-lipase complex is more efficacious in opening a new pathway for lipolysis [65]. Rather than hindering digestion, the high concentration of liberated phospholipids in formulation NEA works alongside bile salts to rapidly encapsulate digested free fatty acids into highly efficient mixed micelles. This rapid micellar clearing prevents product inhibition at the droplet interface, thereby shifting the thermodynamic equilibrium forward to maximize the release of linear free fatty acids. In contrast, formulations with higher synthetic fractions, such as NEC (1.2% w/w Tween 20), reached an early lipolysis plateau (59.89%). This counter-performance occurs because Tween 20 forms highly dense, hydrophilic polyoxyethylene brush barriers around the nano- droplets. Owing to the steric hindrance, Tween 20 competitively sequesters available bile salts and displaces the pancreatic lipase–colipase complex from the oil-water interface [66,67]. This competitive inhibition reduces enzyme accessibility, leading to the saturation and lower digestion rates observed in NEC.

3.9. Confocal laser scanning microscopy images: fate of nanoemulsions in different phases of digestion

Nanoemulsions often undergo morphological and structural changes during digestion [68,69]. Confocal laser scanning microscopy was used to observe these changes and to monitor the size of emulsified oil droplets throughout the digestion period. No significant changes in droplet size or structure were observed in confocal images during the initial stages of digestion in the mouth, indicating that all three formulations remained stable in the simulated oral phase (Fig. 9). The NE system was shown to be sufficiently resistant to droplet aggregation; however, a limited degree of coalescence or flocculation was unavoidable due to the acidic pH of the simulated gastric phase. An increase in droplet diameter and subsequent destabilization of the surfactant layer surrounding the lipid droplets at acidic pH were observed for all formulations, and the presence of several large, clustered structures of droplets in the gastric phase was more evident in the NEA formulation, as indicated by the confocal micrographs (Fig. 9). However, the individual nano-droplets remain intact within these clusters, held together by a tight, viscoelastic multi-lamellar asolectin framework that acts as a physical shield. Because the droplets are clustered rather than merged into a bulk macro-oil phase, the underlying core nanostructure and its high surface-area-to-volume ratio are successfully preserved. Sesame oil lignans (such as sesamol, sesamin, and sesamolin) are prone to chemical alteration when exposed directly to the highly acidic aqueous gastric juice. By packing into large, dense flocs in the gastric matrix, the available surface area exposed to the highly destructive, highly acidic aqueous continuum is drastically minimized. The hydrophobic core of these thick, flocculated clusters creates a restricted microenvironment that traps the lipophilic lignans deep inside the oil droplets. Again, because gastric lipase has a strong preference for short- and medium-chain triglycerides and is highly restricted by tight phospholipid barriers, the sesame oil experiences minimal premature lipolysis or active compound leaking during the simulated mouth and gastric phases.

The ultimate proof that this gastric destabilization does not compromise targeted delivery is evident in the subsequent simulated intestinal-phase data, in which the system undergoes an elegant structural reversal. As confirmed by our intestinal confocal images (Fig. 9), the large gastric clusters dissolve into an abundance of tiny, uniform digested structures, thereby validating the maximum release of free fatty acids from the NEs during the intestinal phase. Thus, the confocal micrographs successfully elucidate a highly efficient, targeted intestinal delivery pathway for the oral formulations.

4. Conclusion

Our rigorous efforts have successfully achieved the objective of the present study, namely, the fabrication of a stable and biocompatible sesame oil NE using a food-grade emulsifier and the optimization of an innovative technology that combines high-speed homogenization and solvent evaporation as an energy-efficient and cost-effective approach. System NEA was formulated to maximize the use of natural biomaterials while minimizing reliance on synthetic commercial surfactants, thereby directly addressing the food industry's push for cleaner labels and reduced additive toxicity. The dense phospholipid scaffold provided the greatest protection against lipid oxidation and facilitated the maximum degree of lipid hydrolysis. Conversely, System NEC was engineered to test the limits of environmental robustness by shifting the balance heavily toward a small-molecule non-ionic surfactant. In NEC, these chains form a dense, brush-like steric barrier around the oil droplets. Because steric stabilization is fundamentally independent of electrostatic screening, NEC maintained exceptional physical stability against intense environmental stressors. System NEB serves as the critical physicochemical midpoint, bridging the structural benefits of both components. This intermediate structure provided moderate shelf-life

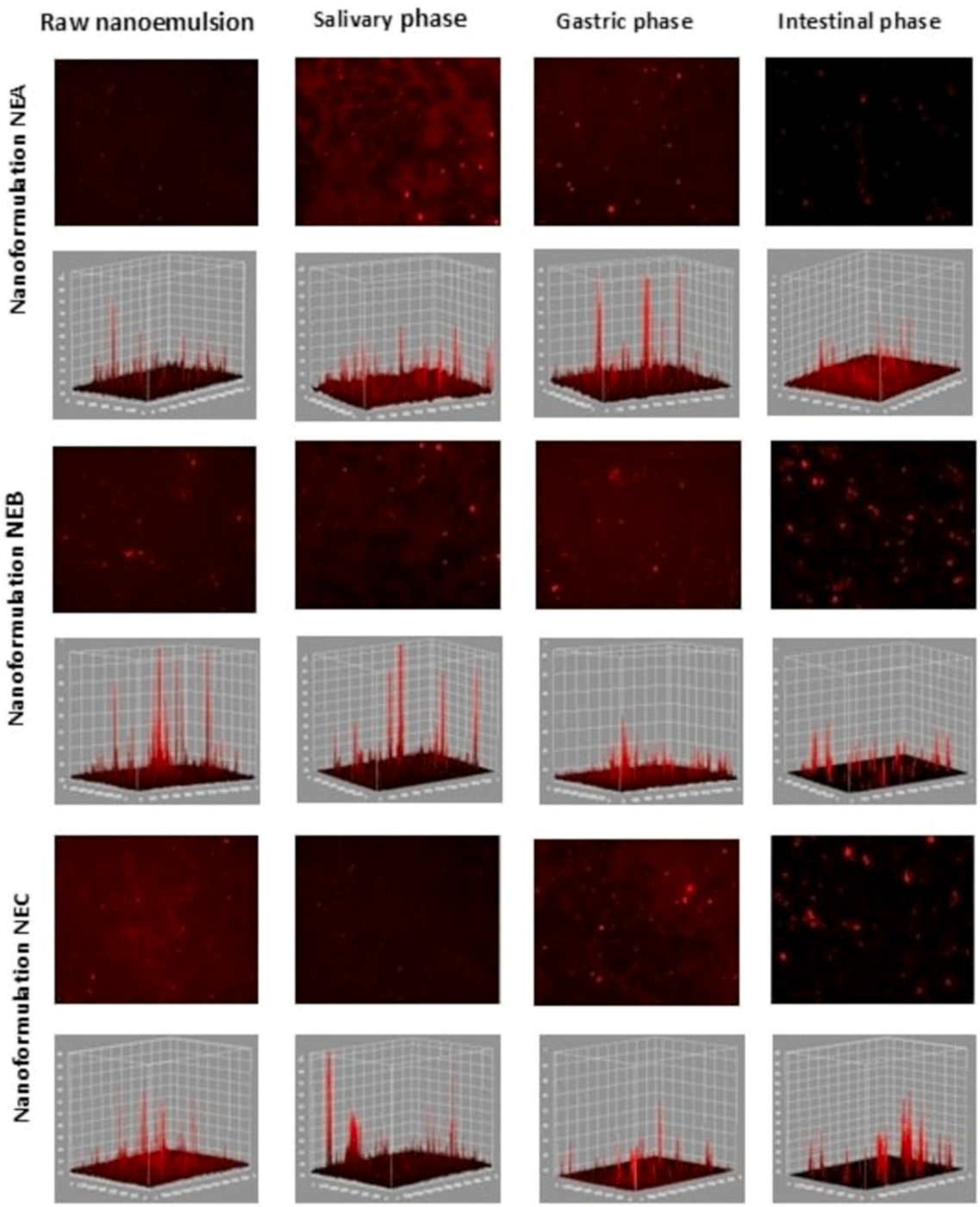


Fig. 9. Confocal Microscopy Images indicating the digestive fate of the formulated nanoemulsions NEA, NEB, and NEC in different phases of simulated digestion.

stability, adequate protection from lipid peroxidation, and an intermediate gastrointestinal digestion profile, making it a highly adaptable baseline control for food matrices requiring broad functionality. Our research is expected to yield both challenging opportunities and satisfactory possibilities in the frontier area of nano-delivery.

Funding

ICMR [Indian Council of Medical Research- File No: 5/9/1212/2019-Nut ICMR; 5/9/1333/2020-Nut] and Council of Scientific and Industrial Research [File No: 09/028(0962)/2015-EMR-I] supported this work.

CRediT authorship contribution statement

Amrita Chakraborty: Writing – original draft, Investigation, Formal analysis, Data curation. **Niloy Chatterjee:** Writing – review & editing, Investigation, Formal analysis, Data curation. **Aatrayee Das:** Formal analysis, Data curation. **Sanjit Dey:** Writing – review & editing, Supervision. **Supratim Ghosh:** Writing – review & editing, Formal analysis, Data curation. **Pubali Dhar:** Writing – review & editing, Validation, Supervision, Project administration, Funding acquisition, Conceptualization.

Acknowledgements

The authors would like to thank Dr Tanmoy Kumar Dey, Dr Sayani Mukherjee, Dr Debjyoti Paul, Dr Arpita Banerjee, Dr Madhushrita Das, Trina Das, and Srija Pal for their assistance in the investigation, formal analysis, data curation and manuscript preparation. We would also like to express our sincere gratitude to the authorities of CRNN, University of Calcutta, for their instrumental support in conducting the research work.

Declaration of Competing Interest

The authors declare that a patent **(patent No. 553136; application No. 202431006963)** has been granted for an invention entitled '**Method of preparation of a novel sesame oil nano emulsion formulation**' for the term of 20 years from the 1st day of February 2024. Furthermore, they declare that they have no known competing financial interests or personal relationships that could be perceived as influencing the work reported in this paper.

Appendix A. Supporting information

Supplementary data associated with this article can be found in the online version at doi:10.1016/j.nxnano.2026.100809.

Data availability

Data will be made available on request.

References

[1] Sambhakar S. Preeti, R. Malik, S. Bhatia, A. Al Harrasi, C. Rani, R. Saharan, S. Kumar, Geeta, R. Sehrawat, Nanoemulsion: an emerging novel technology for improving the bioavailability of drugs, Scientifica 2023 (1) (2023) 6640103, https://doi.org/10.1155/2023/6640103.

[2] T. Das, N. Chatterjee, A. Chakraborty, A. Banerjee, S.B. Haiti, S. Datta, H. Chattopadhyay, P. Dhar, Fabrication of rice bran oil nanoemulsion and conventional emulsion with Mustard Protein Isolate as a novel excipient: focus on shelf-life stability, lipid digestibility and cellular bioavailability, Food Hydrocoll. Health 4 (2023 Dec 15) 100143, https://doi.org/10.1016/j.fhfh.2023.100143.

[3] D.J. McClements, A.K. Das, P. Dhar, P.K. Nanda, N. Chatterjee, Nanoemulsion-based technologies for delivering natural plant-based antimicrobials in foods, Front. Sustain. Food Syst. 5 (2021 Feb 18) 643208, https://doi.org/10.3389/fsufs.2021.643208.

[4] M. Zhang, Q. Cao, Y. Yuan, X. Guo, D. Pan, R. Xie, X. Ju, Z. Liu, W. Wang, L. Chu, Functional nanoemulsions: controllable low-energy nanoemulsification and advanced biomedical application, Chin. Chem. Lett. 35 (2) (2024 Feb 1) 108710, https://doi.org/10.1016/j.cclet.2023.108710.

[5] S. Jacob, F.S. Kather, S.H. Boddu, J. Shah, A.B. Nair, Innovations in nanoemulsion technology: enhancing drug delivery for oral, parenteral, and ophthalmic applications, Pharmaceutics 16 (10) (2024 Oct 17) 1333, https://doi.org/10.3390/pharmaceutics16101333.

[6] J.S. Komaiko, D.J. McClements, Formation of food-grade nanoemulsions using low-energy preparation methods: a review of available methods, Compr. Rev. Food Sci. Food Saf. 15 (2) (2016 Mar) 331–352, https://doi.org/10.1111/1541-4337.12189.

[7] S.J. Lee, D.J. McClements, Fabrication of protein-stabilized nanoemulsions using a combined homogenization and amphiphilic solvent dissolution/evaporation approach, Food Hydrocoll. 24 (6-7) (2010 Aug 1) 560–569, https://doi.org/10.1016/j.foodhyd.2010.02.002.

[8] I.R. Singh, A.K. Pulikkal, Nano emulsions stabilized by natural emulsifiers: a comprehensive review on feasibility, stability and bio-applicability, J. Drug. Deliv. Sci. Technol. 92 (2024 Feb 1) 105303, https://doi.org/10.1016/j.jddst.2023.105303.

[9] Y. Jin, A. Adhikari, Recent developments and applications of food-based emulsifiers from plant and animal sources, Colloids Interfaces 9 (5) (2025 Sep 10) 61, https://doi.org/10.3390/colloids9050061.

[10] J.M. Andersson, O. Masbernat, K. Roger, Emulsions stabilized by phospholipids, J. Colloid Interface Sci. 678 (2025 Jan 15) 410–418, https://doi.org/10.1016/j.jcis.2024.08.249.

[11] C.N. Pereira Oliveira, M. Nani Leite, N.A. de Paula, Y. Araújo Martins, S. A. Figueiredo, M.A. Cipriani Frade, R.F. Lopez, Nanoemulsions based on sunflower and rosehip oils: the impact of natural and synthetic stabilizers on skin penetration and an ex vivo wound healing model, Pharmaceutics 15 (3) (2023 Mar 20) 999, https://doi.org/10.3390/pharmaceutics15030999.

[12] L.C. Velasco-Rodríguez, A.A. Esperón-Rojas, C. Cano-Sarmiento, M.P. Rascón-Díaz, H.S. García, Kinetic stability and bioavailability of curcumin nanoemulsions stabilized with krill oil phospholipids, Food Biosci. 62 (2024 Dec 1) 105200, https://doi.org/10.1016/j.fbio.2024.105200.

[13] Y.R. Tang, S. Ghosh, Stability and rheology of canola protein isolate-stabilized concentrated oil-in-water emulsions, Food Hydrocoll. 113 (2021 Apr 1) 106399, https://doi.org/10.1016/j.foodhyd.2020.106399.

[14] P.K. Arya, A. Jindal, A. Kumar, Cytotoxicity potential of basil oil embedded 5-fluorouracil-phospholipid complex loaded self-nanoemulsifying system: design expert® endorsed approach for bioavailability enhancement, J. Mol. Liq. (2025 Dec 2) 129021, https://doi.org/10.1016/j.molliq.2025.129021.

[15] A. Jindal, A. Saifi, A. Kumar, D. Chaudhary, Quality by design (QbD) accredited rutin-loaded self-nanoemulsifying system of Krill oil for improved dissolution rate, ameliorating human neuroblastoma and hyperlipidemia, Int. J. Biol. Macromol. 320 (2025 Aug 1) 145768, https://doi.org/10.1016/j.ijbiomac.2025.145768.

[16] N. Chatterjee, S. Pal, P. Dhar, Green silver nanoparticles from bacteria-antioxidant, cytotoxic and antifungal activities, Nanotechnology 6 (2024 Jan 1) 100089, https://doi.org/10.1016/j.nxnano.2024.100089.

[17] G.M. Huber, H.V. Rupasinghe, F. Shahidi, Inhibition of oxidation of omega-3 polyunsaturated fatty acids and fish oil by quercetin glycosides, Food Chem. 117 (2) (2009 Nov 15) 290–295, https://doi.org/10.1016/j.foodchem.2009.04.007.

[18] Y. Liu, C. Liu, S. Zhang, J. Li, H. Zheng, H. Jin, J. Xu, Comparison of different protein emulsifiers on physicochemical properties of β-carotene-loaded nanoemulsion: effect on formation, stability, and in vitro digestion, Nanomaterials 11 (1) (2021 Jan 11) 167, https://doi.org/10.3390/nano11010167.

[19] P. Pinsirodom, K.L. Parkin, Lipase assays, C3-1, Curr. Protoc. Food Anal. Chem. (1) (2001), https://doi.org/10.1002/0471142913.fac0301s00.

[20] A.C. Pinheiro, M. Lad, H.D. Silva, M.A. Coimbra, M. Boland, A.A. Vicente, Unravelling the behaviour of curcumin nanoemulsions during in vitro digestion: effect of the surface charge, Soft Matter 9 (11) (2013) 3147–3154, https://doi.org/10.1039/C3SM27527B.

[21] V. Agmo Hernández, An overview of surface forces and the DLVO theory, ChemTexts 9 (4) (2023 Jul 22) 10, https://doi.org/10.1007/s40828-023-00182-9.

[22] P. Scholz, C.M. Keck, Nanoemulsions produced by rotor–stator high–speed stirring, Int. J. Pharm. 482 (1-2) (2015 Mar 30) 110–117, https://doi.org/10.1016/j.ijpharm.2014.12.040.

[23] T.J. Wooster, M. Golding, P. Sanguansri, Impact of oil type on nanoemulsion formation and Ostwald ripening stability, Langmuir 24 (22) (2008 Nov 18) 12758–12765, https://doi.org/10.1021/la801685v.

[24] N. Pal, N. Kumar, A. Mandal, Stabilization of dispersed oil droplets in nanoemulsions by synergistic effects of the gemini surfactant, PHPA polymer, and silica nanoparticle, Langmuir 35 (7) (2019 Jan 23) 2655–2667, https://doi.org/10.1021/acs.langmuir.8b03364.

[25] S.J. Lee, S.J. Choi, Y. Li, E.A. Decker, D.J. McClements, Protein-stabilized nanoemulsions and emulsions: comparison of physicochemical stability, lipid oxidation, and lipase digestibility, J. Agric. Food Chem. 59 (1) (2011 Jan 12) 415–427, https://doi.org/10.1021/jf103511v.

[26] I. Fortelný, J. Jůza, Description of the droplet size evolution in flowing immiscible polymer blends, Polymers 11 (5) (2019 Apr 30) 761, https://doi.org/10.3390/polym11050761.

[27] X. Zhang, J. Niu, J.Y. Wu, Evaluation and manipulation of the key emulsification factors toward highly stable PCM-water nano-emulsions for thermal energy storage, Sol. Energy Mater. Sol. Cells 219 (2021 Jan 1) 110820, https://doi.org/10.1016/j.solmat.2020.110820.

[28] A. Kumar, L.V. Singh, S. Singh, Phospholipid-α-tocopherol complexation-based self-nanoemulsifying system: assessment of phase behaviour, lipolysis stability & apoptotic activity, BioNanoScience 15 (2) (2025 Jun) 248, https://doi.org/10.1007/s12668-025-01854-1.

[29] D.J. McClements, J. Rao, Food-grade nanoemulsions: formulation, fabrication, properties, performance, biological fate, and potential toxicity, Crit. Rev. Food Sci. Nutr. 51 (4) (2011 Mar 25) 285–330, https://doi.org/10.1080/10408398.2011.559558.

[30] S.A. McBride, F. Temprano-Coleto, P.R. Kaneelil, R. Knopp, A.J. Taylor, M. A. Storey-Matsutani, J.L. Wilson, M.S. Saleh, A.R. Konicek, A. Jusufi, M. S. Yeganeh, Effect of capillary number and viscosity ratio on multiphase displacement in microscale pores, Phys. Rev. Fluids 10 (5) (2025 May) 054201, https://doi.org/10.1103/PhysRevFluids.10.054201.

[31] V. Klang, C. Valenta, Lecithin-based nanoemulsions, J. Drug. Deliv. Sci. Technol. 21 (1) (2011 Jan 1) 55–76, https://doi.org/10.1016/S1773-2247(11)50006-1.

[32] M.T. Baker, M. Naguib, D.C. Warltier, Propofol: the challenges of formulation, Anesthesiology 103 (4) (2005 Oct 1) 860–876, https://doi.org/10.1097/00000542-200510000-00026.

[33] A. Johns, S. Morris, K. Edwards, R.L. Quirino, Asolectin from soybeans as a natural compatibilizer for cellulose-reinforced biocomposites from tung oil, J. Appl. Polym. Sci. 132 (17) (2015 May 5), https://doi.org/10.1002/app.41833.

[34] L. Rydhag, I. Wilton, The function of phospholipids of soybean lecithin in emulsions, J. Am. Oil Chem. ' Soc. 58 (8) (1981 Aug) 830–837, https://doi.org/10.1007/BF02665591.

[35] S. Hoeller, A. Sperger, C. Valenta, Lecithin-based nanoemulsions: a comparative study of the influence of non-ionic surfactants and the cationic phytosphingosine on physicochemical behaviour and skin permeation, Int. J. Pharm. 370 (1-2) (2009 Mar 31) 181–186, https://doi.org/10.1016/j.ijpharm.2008.11.014.

[36] M. Trotta, F. Pattarino, T. Ignoni, Stability of drug-carrier emulsions containing phosphatidylcholine mixtures, Eur. J. Pharm. Biopharm. 53 (2) (2002 Mar 1) 203–208, https://doi.org/10.1016/S0939-6411(01)00230-2.

[37] J.J. Wang, K.C. Sung, O.Y. Hu, C.H. Yeh, J.Y. Fang, Submicron lipid emulsion as a drug delivery system for nalbuphine and its prodrugs, J. Control. Release 115 (2) (2006 Oct 10) 140–149, https://doi.org/10.1016/j.jconrel.2006.07.023.

[38] L. Dresser, S.P. Graham, L.M. Miller, C. Schaefer, D. Conteduca, S. Johnson, M. C. Leake, S.D. Quinn, Tween-20 induces the structural remodelling of single lipid vesicles, J. Phys. Chem. Lett. 13 (23) (2022 Jun 9) 5341–5350, https://doi.org/10.1021/acs.jpclett.2c00704.
[39] A. Kumar, A. Saifi, A. Sharma, D. Chaudhary, Self-nanoemulsifying pre-concentrate of γ-tocotrienol embedding phospholipid: phase dynamics, anti-hyperlipidemic and anti-neuroblastoma potential, BioNanoScience 15 (3) (2025 Sep) 352, https://doi.org/10.1007/s12668-025-01973-9.
[40] D.J. McClements, S.M. Jafari, General aspects of nanoemulsions and their formulation. Nanoemulsions, Academic Press, 2018 Jan 1, pp. 3–20, https://doi.org/10.1016/B978-0-12-811838-2.00001-1.
[41] N. Riquelme, R.N. Zúñiga, C. Arancibia, Physical stability of nanoemulsions with emulsifier mixtures: replacement of Tween 80 with quillaja saponin, Lwt 111 (2019 Aug 1) 760–766, https://doi.org/10.1016/j.lwt.2019.05.067.
[42] R. Pichot, R.L. Watson, I.T. Norton, Phospholipids at the interface: current trends and challenges, Int. J. Mol. Sci. 14 (6) (2013 Jun 3) 11767–11794, https://doi.org/10.3390/ijms140611767.
[43] M.I. Moran-Valero, V.M. Ruiz-Henestrosa, A.M. Pilosof, Synergistic performance of lecithin and glycerol monostearate in oil/water emulsions, Colloids Surf. b Biointerfaces 151 (2017 Mar 1) 68–75, https://doi.org/10.1016/j.colsurfb.2016.12.015.
[44] A.M. De Toledo, N.C. Silva, A.C. Sato, C.S. Picone, A comprehensive study of physical, antimicrobial and emulsifying properties of self-assembled chitosan/lecithin complexes produced in aqueous media, Future Foods 4 (2021 Dec 1) 100083, https://doi.org/10.1016/j.fufo.2021.100083.
[45] Y. Tan, D. Wannasin, D.J. McClements, Utilization of potato protein fractions to form oil-in-water nanoemulsions: Impact of pH, salt, and heat on their stability, Food Hydrocoll. 137 (2023 Apr 1) 108356, https://doi.org/10.1016/j.foodhyd.2022.108356.
[46] A. Teo, K.K. Goh, J. Wen, I. Oey, S. Ko, H.S. Kwak, S.J. Lee, Physicochemical properties of whey protein, lactoferrin and Tween 20 stabilised nanoemulsions: effect of temperature, pH and salt, Food Chem. 197 (2016 Apr 15) 297–306, https://doi.org/10.1016/j.foodchem.2015.10.086.
[47] W. Gao, Z. Jiang, X. Du, F. Zhang, Y. Liu, X. Bai, G. Sun, Impact of surfactants on nanoemulsions based on fractionated coconut oil: emulsification stability and in vitro digestion, J. Oleo Sci. 69 (3) (2020) 227–239, https://doi.org/10.5650/jos.ess19264.
[48] Z. Zhu, Y. Wen, J. Yi, Y. Cao, F. Liu, D.J. McClements, Comparison of natural and synthetic surfactants at forming and stabilizing nanoemulsions: tea saponin, Quillaja saponin, and Tween 80, J. Colloid Interface Sci. 536 (2019 Feb 15) 80–87, https://doi.org/10.1016/j.jcis.2018.10.024.
[49] G. Wang, T. Wang, Oxidative stability of egg and soy lecithin as affected by transition metal ions and pH in emulsion, J. Agric. Food Chem. 56 (23) (2008 Dec 10) 11424–11431, https://doi.org/10.1021/jf8022832.
[50] S. Uluata, D.J. McClements, E.A. Decker, Physical stability, autoxidation, and photosensitized oxidation of ω-3 oils in nanoemulsions prepared with natural and synthetic surfactants, J. Agric. Food Chem. 63 (42) (2015 Oct 28) 9333–9340, https://doi.org/10.1021/acs.jafc.5b03572.
[51] Y. Pan, R.V. Tikekar, N. Nitin, Effect of antioxidant properties of lecithin emulsifier on oxidative stability of encapsulated bioactive compounds, Int. J. Pharm. 450 (1-2) (2013 Jun 25) 129–137, https://doi.org/10.1016/j.ijpharm.2013.04.038.
[52] L. Cui, E.A. Decker, Phospholipids in foods: prooxidants or antioxidants? J. Sci. Food Agric. 96 (1) (2016 Jan 15) 18–31, https://doi.org/10.1002/jsfa.732.
[53] L. Cui, J. Fan, Y. Sun, Z. Zhu, J. Yi, The prooxidant activity of salts on the lipid oxidation of lecithin-stabilized oil-in-water emulsions, Food Chem. 252 (2018 Jun 30) 28–32, https://doi.org/10.1016/j.foodchem.2018.01.094.
[54] M. Andargie, M. Vinas, A. Rathgeb, E. Möller, P. Karlovsky, Lignans of sesame (Sesamum indicum L.): a comprehensive review, Molecules 26 (4) (2021 Feb 7) 883, https://doi.org/10.3390/molecules26040883.
[55] S. Mun, E.A. Decker, D.J. McClements, Influence of emulsifier type on in vitro digestibility of lipid droplets by pancreatic lipase, Food Res. Int. 40 (6) (2007 Jul 1) 770–781, https://doi.org/10.1016/j.foodres.2007.01.007.
[56] B. Kupikowska-Stobba, H. Niu, I. Klojdová, R. Agregán, J.M. Lorenzo, M. Kasprzak, Controlled lipid digestion in the development of functional and personalized foods for a tailored delivery of dietary fats, Food Chem. 466 (2025 Feb 28) 142151, https://doi.org/10.1016/j.foodchem.2024.142151.
[57] J. Maldonado-Valderrama, P. Wilde, A. Macierzanka, A. Mackie, The role of bile salts in digestion, Adv. Colloid Interface Sci. 165 (1) (2011 Jun 9) 36–46, https://doi.org/10.1016/j.cis.2010.12.002.
[58] Y. Li, M. Hu, D.J. McClements, Factors affecting lipase digestibility of emulsified lipids using an in vitro digestion model: proposal for a standardised pH-stat method, Food Chem. 126 (2) (2011 May 15) 498–505, https://doi.org/10.1016/j.foodchem.2010.11.027.
[59] A. Gasa-Falcon, I. Odriozola-Serrano, G. Oms-Oliu, O. Martín-Belloso, Impact of emulsifier nature and concentration on the stability of β-carotene-enriched nanoemulsions during in vitro digestion, Food & Funct. 10 (2) (2019) 713–722, https://doi.org/10.1039/C8FO02069H.
[60] M. Wickham, M. Garrood, J. Leney, P.D. Wilson, A. Fillery-Travis, Modification of a phospholipid stabilized emulsion interface by bile salt: effect on pancreatic lipase activity, J. Lipid Res. 39 (3) (1998 Mar 1) 623–632, https://doi.org/10.1016/S0022-2275(20)33300-9.
[61] Y. Yang, E.A. Decker, H. Xiao, D.J. McClements, Enhancing vitamin E bioaccessibility: Factors impacting solubilization and hydrolysis of α-tocopherol acetate encapsulated in emulsion-based delivery systems, Food & Funct. 6 (1) (2015) 83–96, https://doi.org/10.1039/C4FO00725E.
[62] P.K. Okuro, M. Viau, S. Marze, S. Laurent, R.L. Cunha, C. Berton-Carabin, A. Meynier, vitro digestion of high-lipid emulsions: towards a critical interpretation of lipolysis, Food & Funct. 14 (24) (2023) 10868–10881, https://doi.org/10.1039/D3FO03816E.
[63] M. Hu, Y. Li, E.A. Decker, D.J. McClements, Role of calcium and calcium-binding agents on the lipase digestibility of emulsified lipids using an in vitro digestion model, Food Hydrocoll. 24 (8) (2010 Nov 1) 719–725, https://doi.org/10.1016/j.foodhyd.2010.03.010.
[64] H. Zheng, W. Wijaya, H. Zhang, K. Feng, Q. Liu, T. Zheng, Z. Yin, Y. Cao, Q. Huang, Improving the bioaccessibility and bioavailability of carnosic acid using a lecithin-based nanoemulsion: complementary in vitro and in vivo studies, Food & Funct. 11 (9) (2020) 8141–8149, https://doi.org/10.1039/D0FO01098G.
[65] A.I. Mulet-Cabero, P.J. Wilde, Role of calcium on lipid digestion and serum lipids: a review, Crit. Rev. Food Sci. Nutr. 63 (6) (2023 Feb 28) 813–826, https://doi.org/10.1080/10408398.2021.1954873.
[66] P. Zhang, Y. Li, Z. Wang, Y. Liu, Z. Ran, Y. Cai, B. Xu, C. Wang, Interfacial mechanisms regulating lipid digestion: a systematic study using tween surfactants with varying structural features, Food Chem. (2025 Aug 15) 145980, https://doi.org/10.1016/j.foodchem.2025.145980.
[67] Y. Li, D.J. McClements, Inhibition of lipase-catalyzed hydrolysis of emulsified triglyceride oils by low-molecular weight surfactants under simulated gastrointestinal conditions, Eur. J. Pharm. Biopharm. 79 (2) (2011 Oct 1) 423–431, https://doi.org/10.1016/j.ejpb.2011.03.019.
[68] D.D. Milinčić, A.S. Salević-Jelić, A.Ž. Kostić, S.P. Stanojević, V. Nedović, M. B. Pešić, Food nanoemulsions: how simulated gastrointestinal digestion models, nanoemulsion, and food matrix properties affect bioaccessibility of encapsulated bioactive compounds, Crit. Rev. Food Sci. Nutr. 64 (22) (2024 Aug 28) 8091–8113, https://doi.org/10.1080/10408398.2023.2195519.
[69] R.F. Gonçalves, J.T. Martins, L. Abrunhosa, A.A. Vicente, A.C. Pinheiro, Nanoemulsions for enhancement of curcumin bioavailability and their safety evaluation: Effect of emulsifier type, Nanomaterials 11 (3) (2021 Mar 23) 815, https://doi.org/10.3390/nano11030815.